Nearly Normal Galaxies 3: Spiral Galaxies

- Many of the properties of spiral galaxies have been previous discussed
- Star formation in galaxies, much of which is occuring in spiral galaxies, will be discussed in the next section
- Present focus: structure of spiral galaxies and dynamics of disk structure

Review of Properties Previously Discussed

- Spiral galaxies are comprised of a bulge & disk component
- Bulge → old stars   Disk → young stars
- The disk contains a large quantity of gas & dust
- M_B ~ -18 to -24
- M / L_V ~ 4
- Disks are cold (rotationally supported) may be important to maintain spiral structure
- The rotation curves of spiral galaxies rise like a solid body in the central regions, then flatten out (i.e., $v(r)$ = constant). This flattening is due to the presence of a dark matter halo.

Trends with Hubble Type (Previously discussed)

- Total luminosity ↓ with ST (Sa → Sc)
- M / L_B ↓ with ST (i.e., young stars have low M / L_B)
- M (HI) / M (total) ↑ with ST (S0 → Sm, Irr)
- M / L_B ↓ as (B – V) ↓ (i.e., because red stars = early type & blue stars = late type)
- Bulge / Disk ↑ with increasing Hubble Type
- Tightness of the spiral arms ↓ with increasing Hubble Type
- Degree to which the arms are resolved into stars & individual emission nebulae (HII regions) ↑ with Hubble Type

Profiles

The profiles of spiral galaxies are a combination of an Inner r¼ - law bulge & an outer exponential disk,

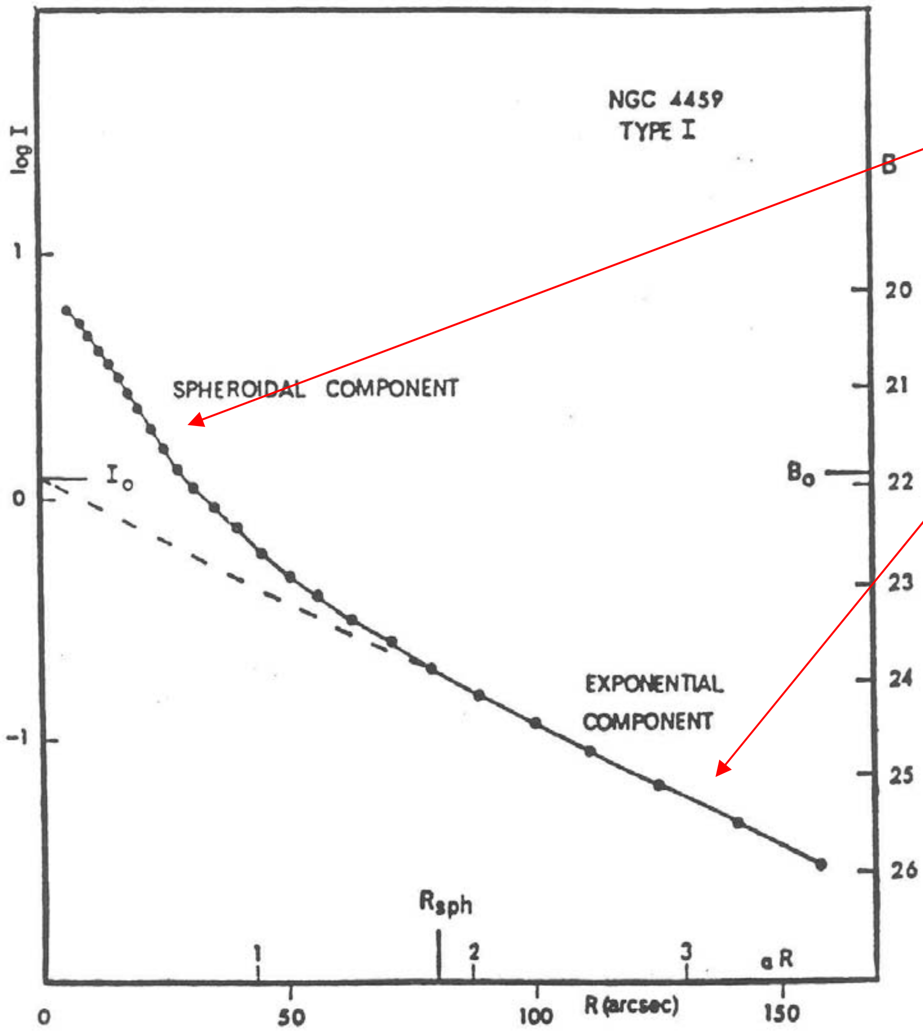

$$log I \propto R^{1/4} \quad \text{(inner);}$$

$$I(R) = I_0 e^{-\alpha r} \quad \text{(outer)}$$

Once again, α is the inverse scale height

(Freeman 1970)

α^{-1} ↓ as S0 → Im

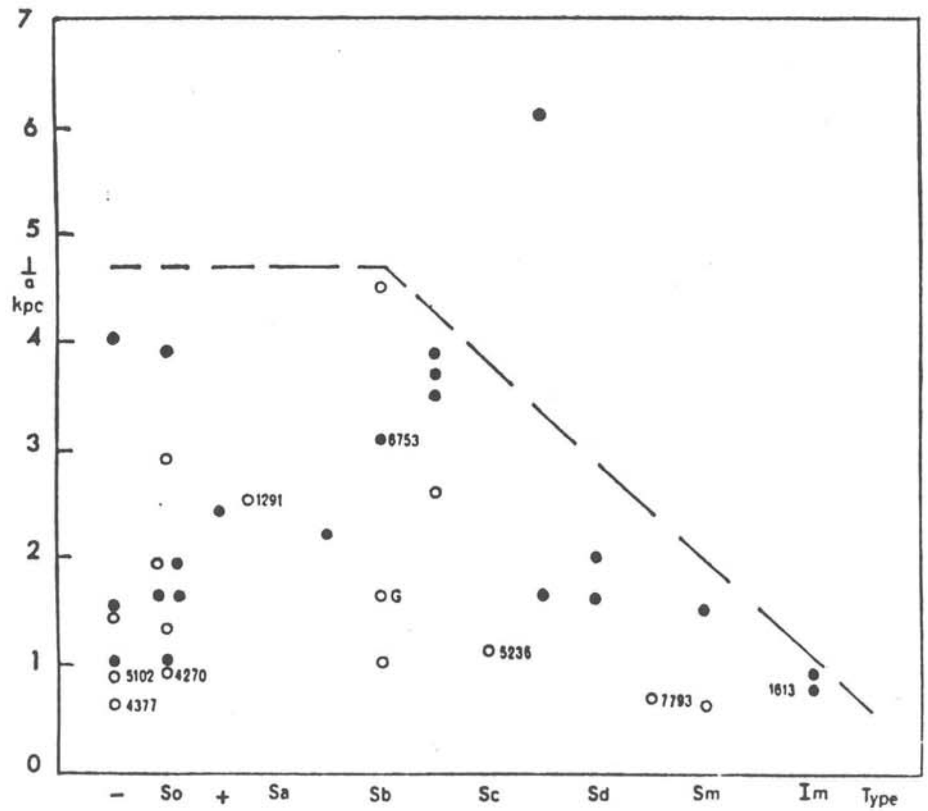

FIG. 6.—Length scale α^{-1} (kpc) for the exponential disks of thirty-six galaxies against their type. NGC numbers are shown for systems defined in Figure 5. *Filled circles*, Type I luminosity profile; *open circles*, Type II luminosity profile (see Fig. 1). *Broken line*, apparent upper envelope. *G* denotes an estimate for the Galaxy.

$\alpha^{-1} \approx 1 - 5$ kpc

(Freeman 1970)

Intrinsic Blue Surface Brightness

$B(0)_c$
(mag arcsec^{-2})

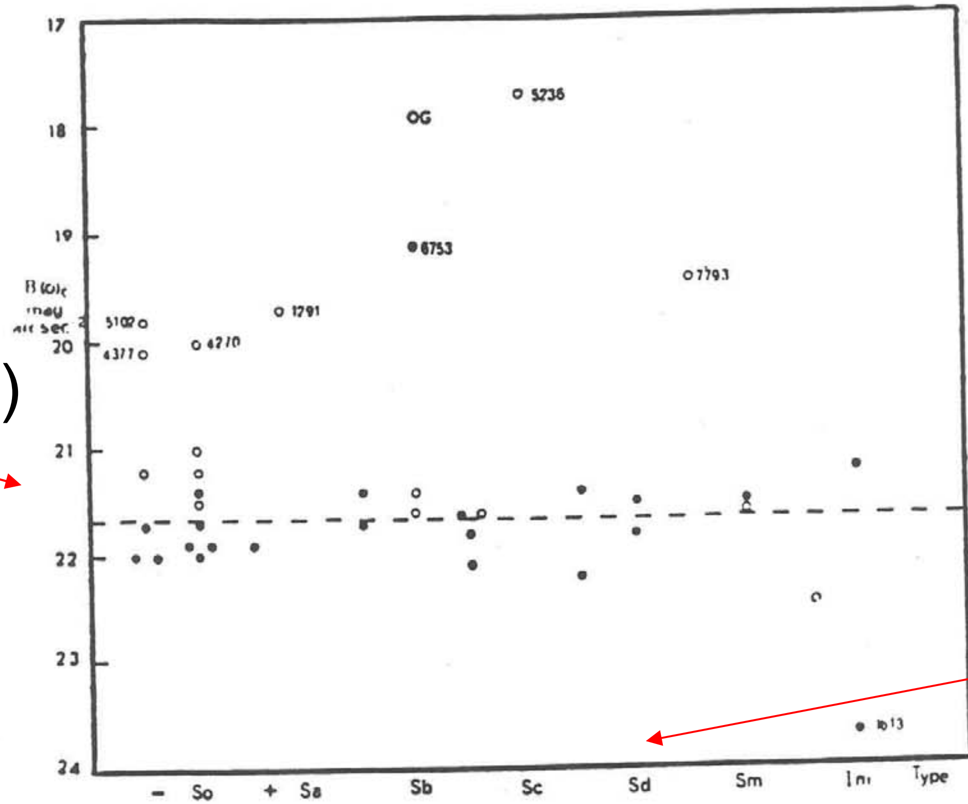

Hubble
Type

FIG. 5.—Intrinsic distance-independent blue-light luminosity scale $B(0)_c$ for the exponential disks of thirty-six galaxies against their morphological type. Broken line at $B(0)_c = 21.65$ is the mean for twenty-eight galaxies. NGC numbers are shown for the other eight. G denotes an estimate for the Galaxy. *Filled circles*, Type I luminosity profile; *open circles*, Type II luminosity profile (see Fig. 1).

$\boxed{B(0)_c \approx \text{constant.}}$ We will return to this soon.

(Freeman 1970)

Departures from an Exponential Disk Profile

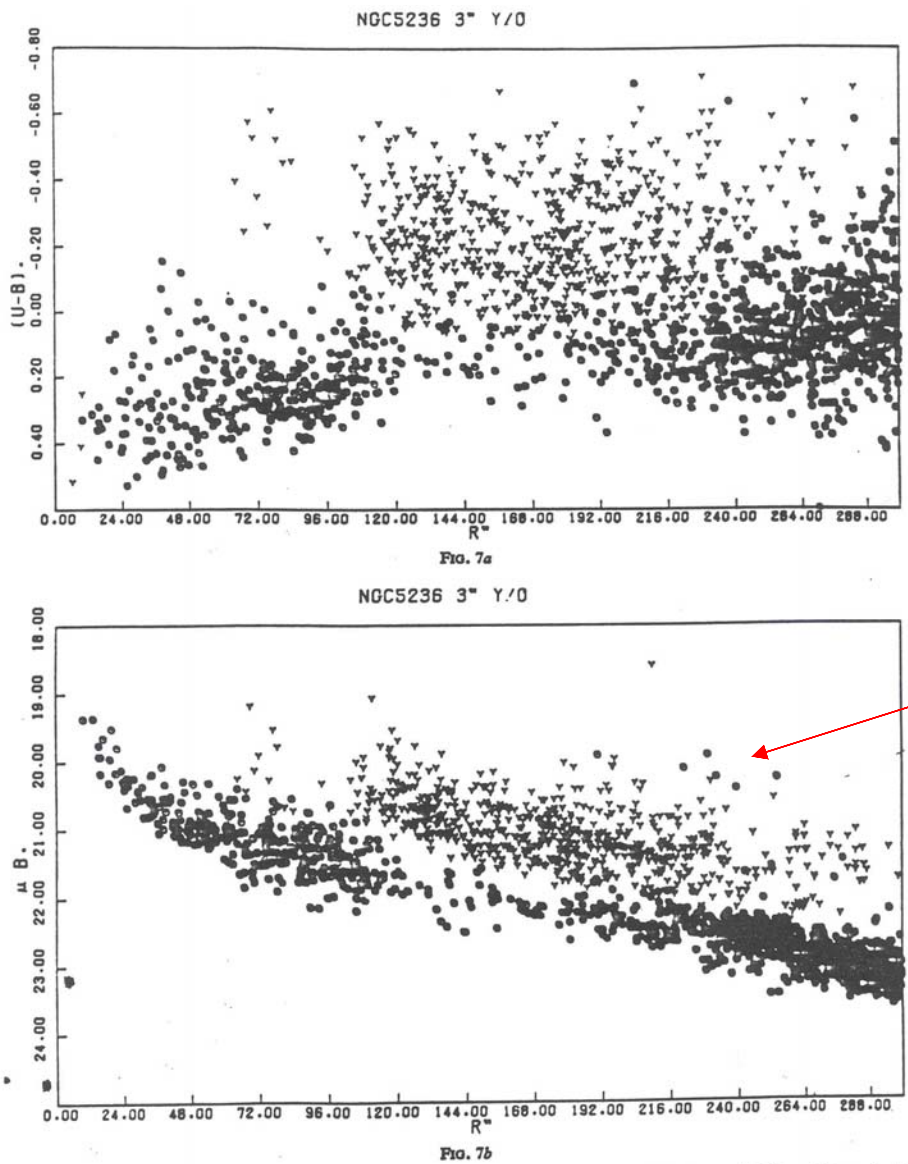

FIG. 7.—(a) $(U-B)_0$; (b) μ_{B0}, for pixels selected on the basis of their color. "Old light" pixels $[(B-V)_0 > 0.65]$ are shown as O's, and "young light" pixels $[(B-V)_0 < 0.40]$ are shown as Y's.

1) might be due to regions of recent Star Formation

Blue Pixels are contributing to non-exponential Disk

(Talbot, Jensen & Dufour 1979)

Departures: 2) Presence of Lens recent made by resonance (bar) destruction

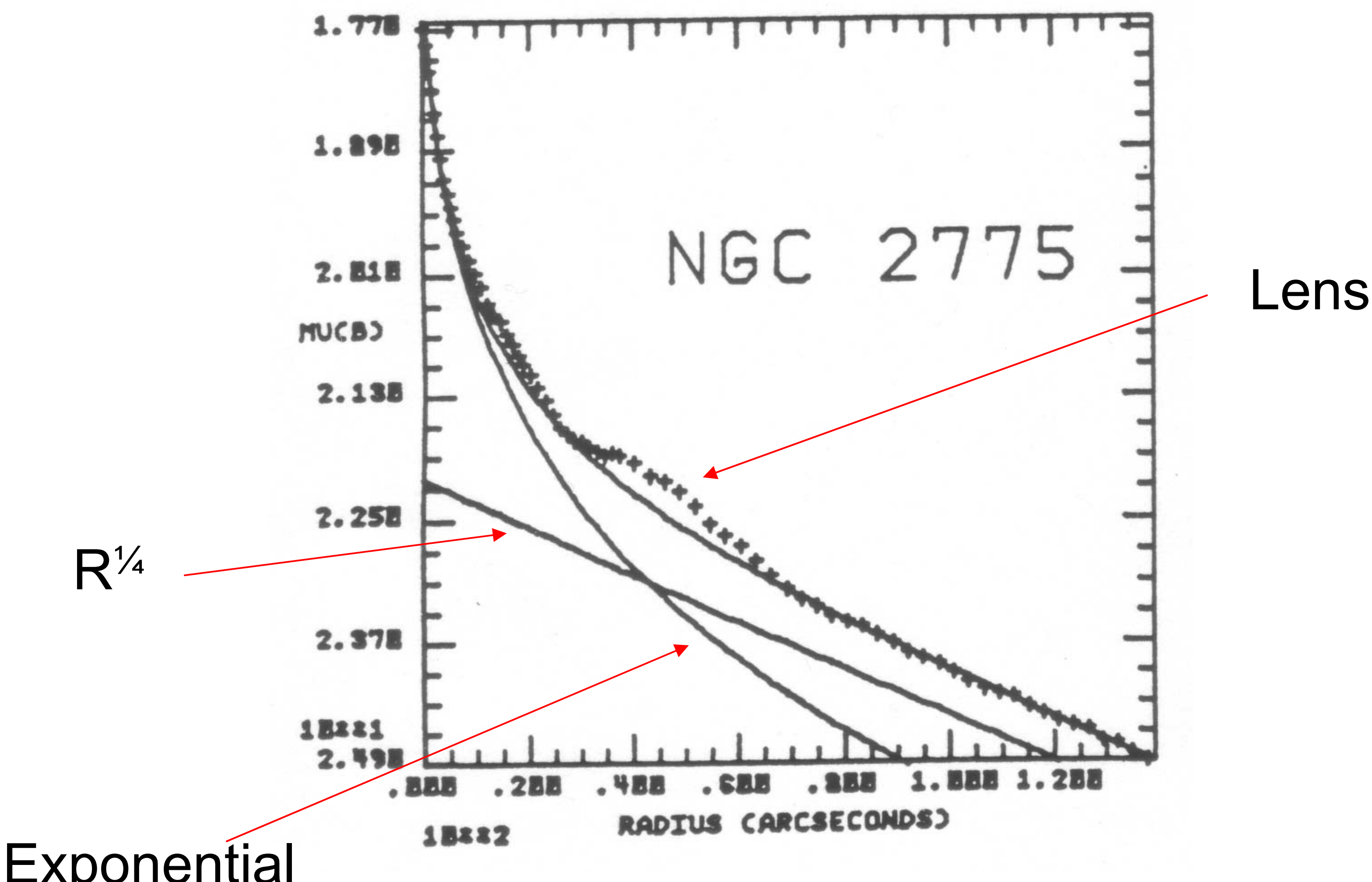

Departures: 3) Bulges that are really disks

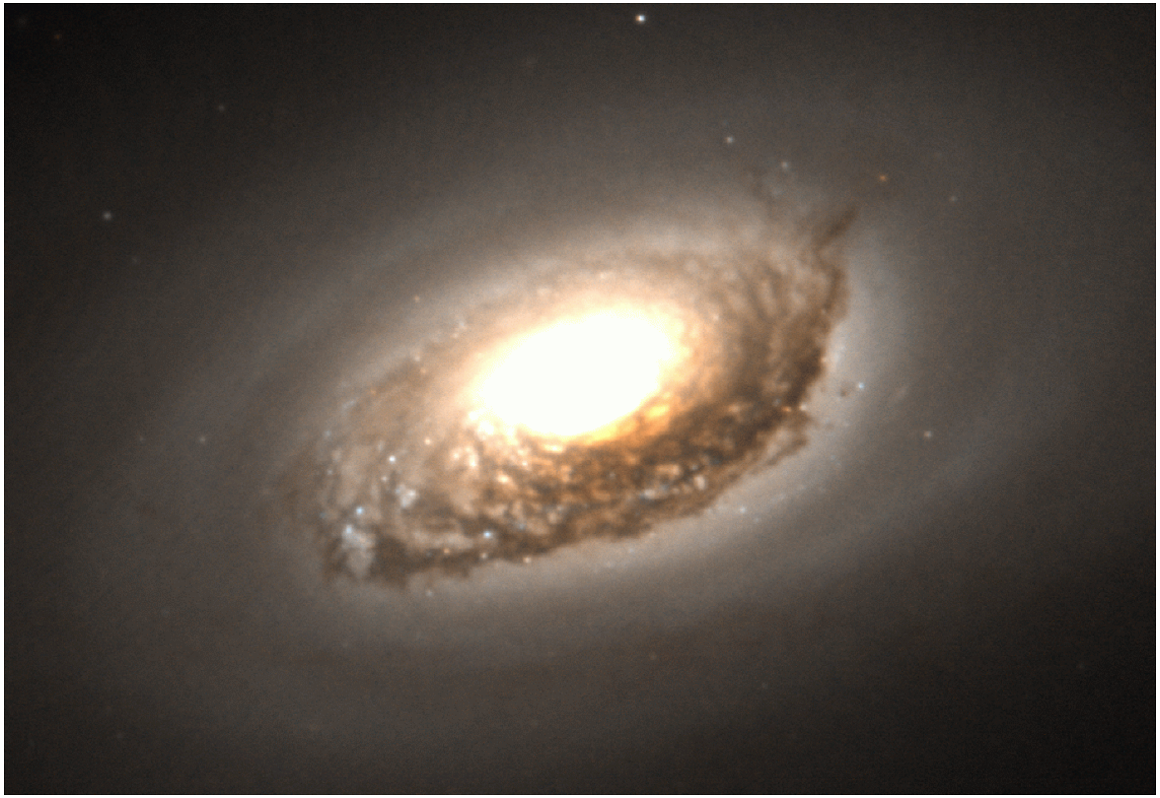

- They can be fitted by an $r^{1/4}$ profile, but have spiral structure & $(v / \sigma)^*$ consistent with rotation
- You can make a bulge by transporting gas inward & igniting a nuclear starburst.

Departures: 4) Thick Disk

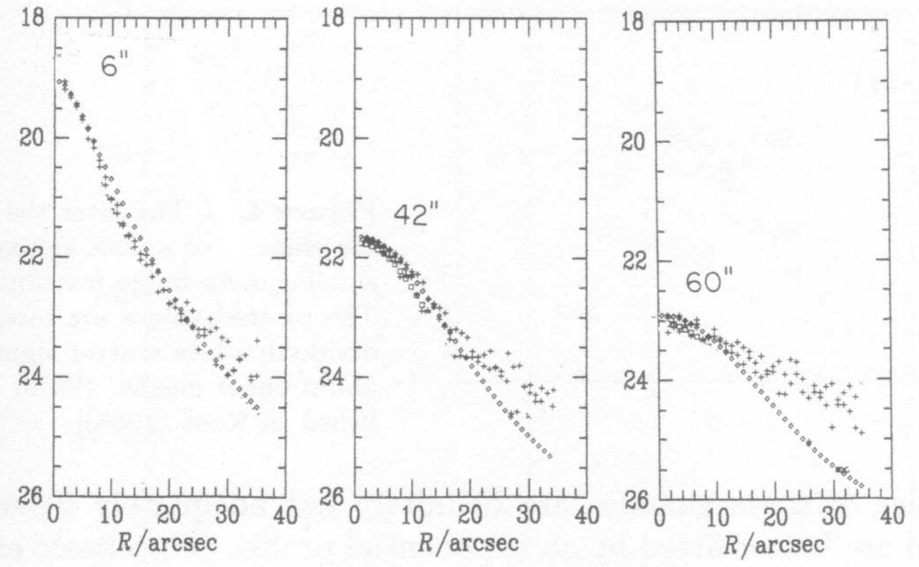

Figure 4.50 Perpendicular profiles of NGC 4350 at major-axis intercepts $R = 6''$, $R = 42''$, $R = 60''$ [After Burstein (1979) courtesy of D. Burstein]

- Have intermediate flattening between that of a thin disk and a bulge
- Are more diffuse than thin disk
- Have a shallow luminosity gradient parallel to the major axis
- Have a rectangular box shape in thick disk galaxies seen edge-on

Thick Disk Formation

- Intermediate Dissipation
- Dynamical Heating
- A merger which partially destroyed the thin disk through heating

Mass & Luminosity

The central mass surface density can be written as,

$$\Sigma_0 = \frac{M}{L} I_0,$$

where I_0 is the central surface brightness. Because *M/L* is constant with radius, the surface brightness profile,

$$I(R) = I_0 e^{-r/r_0},$$

can be written be written in terms of the mass surface density as,

$$\Sigma(R) = \Sigma_0 e^{-r/r_0}.$$

For a sheet model of a disk, we can write,

$$\frac{dM(r)}{dr} = 2\pi r \Sigma.$$

Mass & Luminosity, cont’

Integrating M (r) from 0 to r,

$$M(r) = 2\pi \int_0^r r\Sigma_0 e^{-r/r_0} dr = 2\pi\Sigma_0 r_0^2 \left[1 - \left(1 + \frac{r}{r_0}\right) e^{-r/r_0}\right].$$

As r $\longrightarrow \infty$,

$$M(\infty) = 2\pi\Sigma_0 r_0^2.$$

Similarly,

$$L(\infty) = 2\pi I_0 r_0^2.$$

We can write,

$$L(\infty) = 2\pi I_0 r_0^2.$$

in terms of M_B,

$$2.5 \log I = 2.5 \log(2\pi I_0) + 2.5 \log r_0^2;$$

$$-M_B = \text{constant} + 5 \log r_0.$$

Once again, the important thing is that I_0 = constant with Hubble Type.

M_B vs. α^{-1}

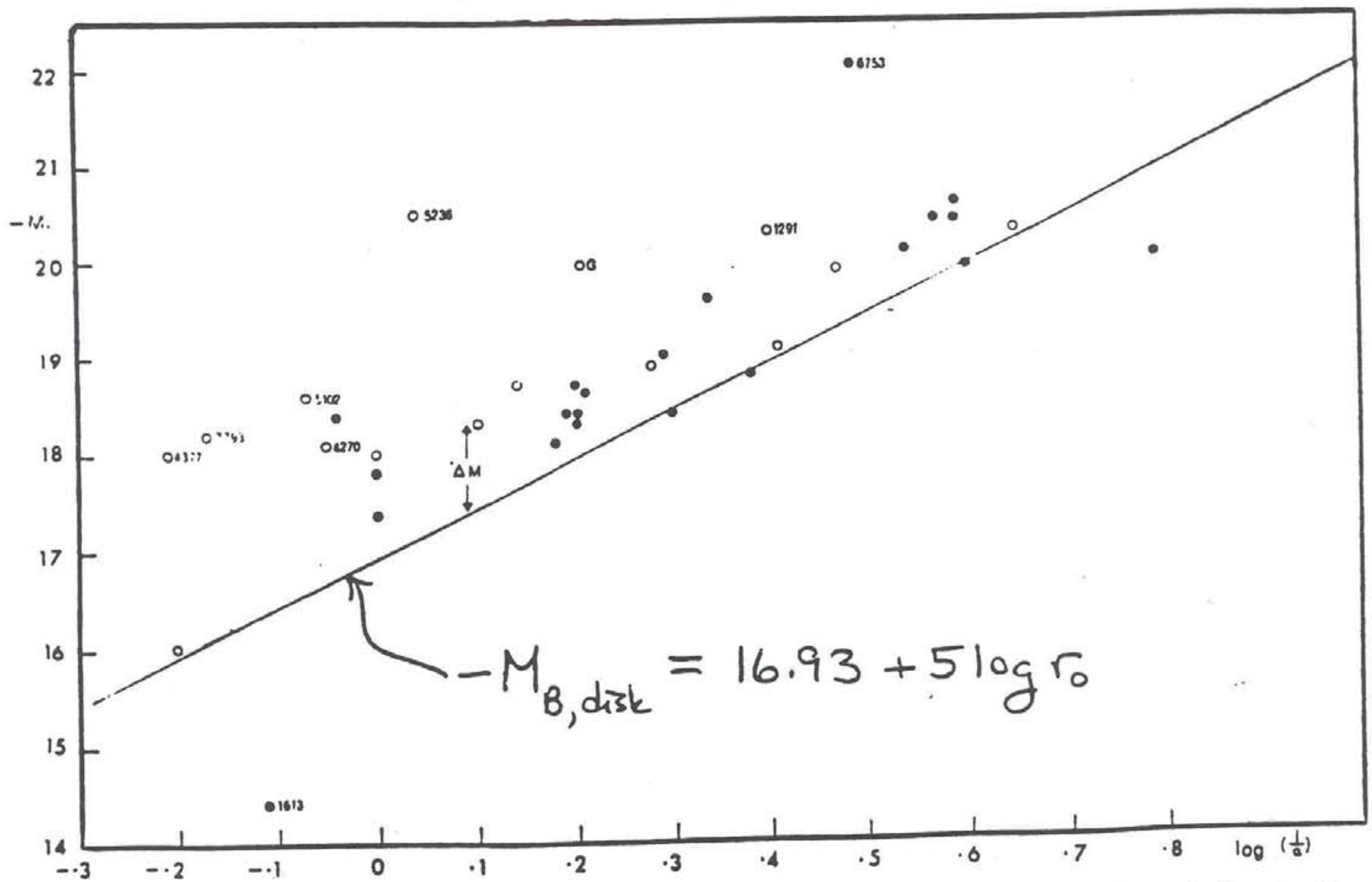

Fig. 7.—Absolute magnitude M_B against the logarithm of the length scale α^{-1} (kpc). Straight line represents $[M_B, \log(\alpha^{-1})]$-relation for exponential disks with $B(0)_c = 21.65$ mag per square second of arc; see eq. (22). Coding is same as for Fig. 6.

$\alpha^{-1} \downarrow$ as M_B

(Freeman 1970)

Total Angular Momentum

The total angular momentum of a disk can be approximated by first considering stars in circular orbits at the scale length radius r_0,

$$\frac{v^2}{r_0} \approx \frac{GM}{r_0^2},$$

which can be rewritten as,

$$v \approx \left(\frac{GM}{r_0}\right)^{1/2}.$$

It turns out that the total angular momentum is approximately equal to,

$$H \approx Mvr_0 = M\left(\frac{GM}{r_0}\right)^{1/2} r_0 \approx (GM^3 r_0)^{1/2}.$$

The actual equation derived by Freeman (1970) for a rotating exponential disk is,

$$H = 1.109\left(GM^3 r_0\right)^{1/2}.$$

Faber-Jackson Relation for Elliptical Galaxies

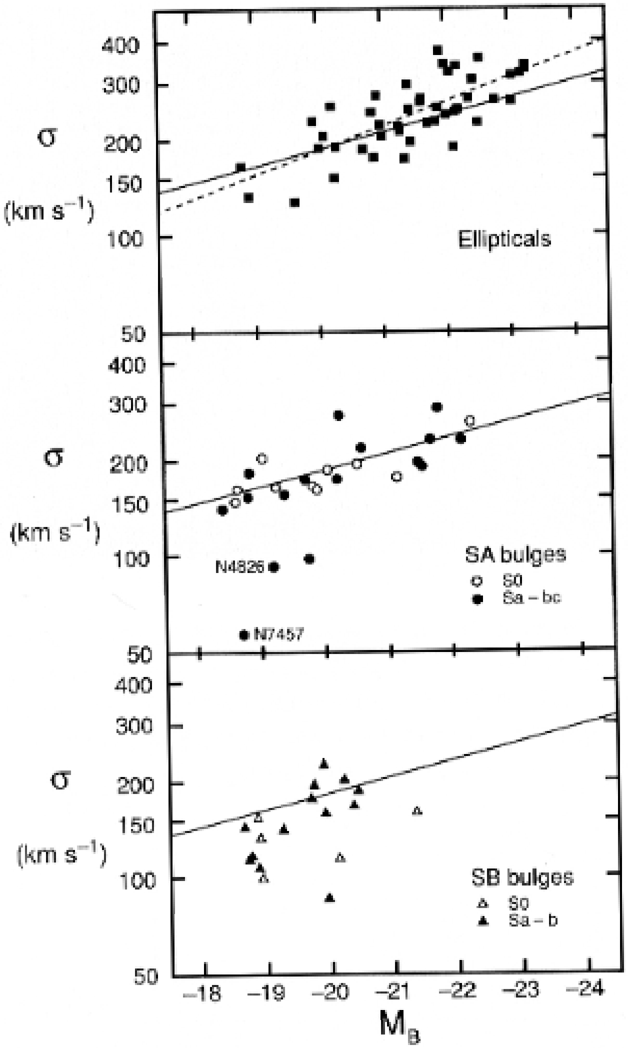

$L \sim \sigma^4(0)$

Fig. 6. Correlation between central velocity dispersion σ and absolute magnitude M_B for elliptical galaxies and for bulges of unbarred (SA) and barred (SB) disk galaxies. The solid line is a fit to the galaxies in the middle panel; the dashed line is a fit to the ellipticals. Except for the NGC 4826 point, this figure is from Kormendy and Illingworth (1983).

Tully-Fisher Relation

I.e., the Faber-Jackson Relation for spiral galaxies. It makes use of HI rotation curves in order to trace the kinematics of spiral galaxies.

Assume stars in circular orbits,

$$v^2 \sim \frac{GM}{r_0};$$

And express the luminosity, *L*, as,

$$L \sim I_0 r_0^2.$$

Squaring the velocity equation, then making the appropriate substitutions,

$$v^4 \sim \frac{G^2M^2}{r_0^2} \sim \frac{G^2M^2I_0}{L}.$$

Solving for *L* yields,

$$L \propto \frac{v^4}{I_0(M/L)^2} \propto v^4.$$

Determining Parameters for Tully Fisher Relation

- Determine distances to a sample of spiral galaxies using other methods
- Observe the sample of spirals in HI. From the velocity curve, determine the full width of the HI at 20% the maximum flux density
- Take out inclination & random disk motion effects in order to get $\Delta v = W_R$,

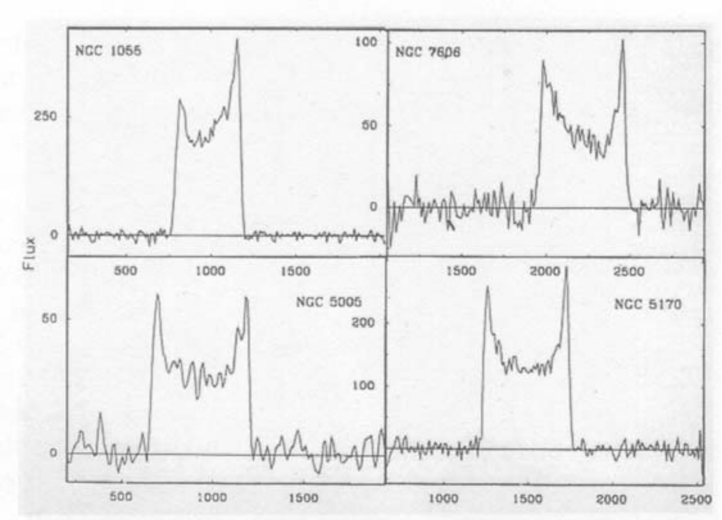

$$W_R = \frac{(W_{\mathrm{FW20M}} - W_{\mathrm{random}})}{\sin i}.$$

Tully-Fisher Relation

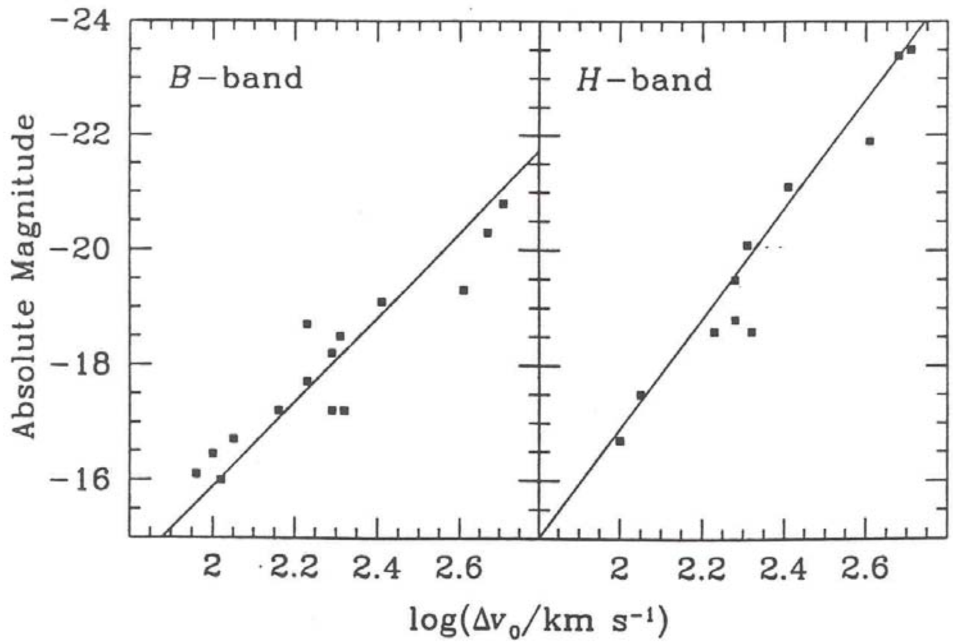

Figure 7.6 Plot of absolute magnitude in B- and H- bands as a function of velocity width for galaxies with independently determined distances. [From the data published in Pierce & Tully (1992)]

$$M_B^i = -7.48(\log W_R^i - 2.50) - 19.55 + \Delta_B \pm 0.14,$$

$$M_R^i = -8.23(\log W_R^i - 2.50) - 20.46 + \Delta_R \pm 0.10,$$

$$M_I^i = -8.72(\log W_R^i - 2.50) - 20.94 \pm 0.10,$$

$$M_H^i = -9.50(\log W_R^i - 2.50) - 21.67 \pm 0.08.$$

Tully-Fisher: $L \rightarrow \Delta v^4$ at Longer λs

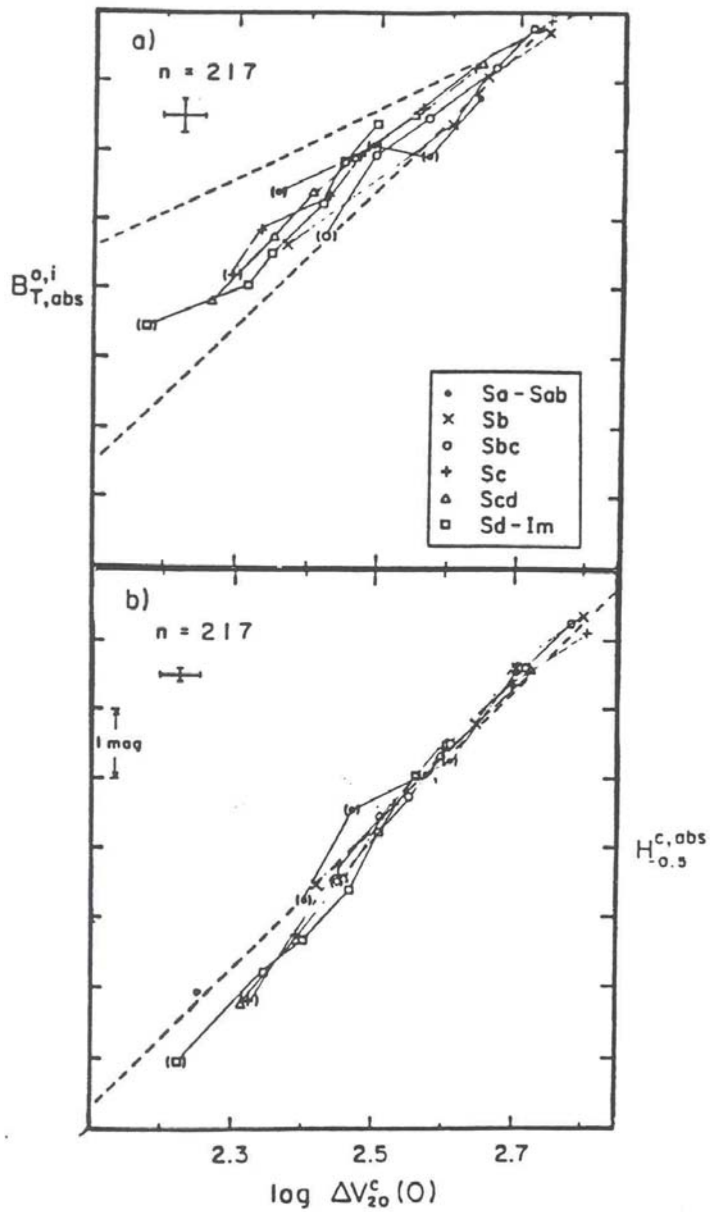

I.e, because $M / L_{\lambda > 0.8\mu m}$ is

1) sensitive to light from older stars
2) less sensitive to dust

FIGURE 12.7
The Tully–Fisher relation in the optical (B, top) and the near IR (H, bottom). The sample of 217 galaxies has been binned using regressions of the two variables, and morphological types are distinguished by different symbols. The lines have slopes corresponding to α = 2 and 4 in Eq. (12.29), but at H only the latter is shown. The absolute-magnitude scales are arbitrary (that is, independent of the actual Hubble constant), and distances have been calculated using a Virgocentric inflow model. (From Aaronson and Mould 1983.)

Dynamics of the Self-Gravitating Isothermal Sheet

Poisson's Equation in cylindrical polar coordinates is,

$$\frac{1}{R}\frac{\partial}{\partial R}\left(R\frac{\partial \Phi}{\partial R}\right)+\frac{1}{R^2}\frac{\partial^2 \Phi}{\partial \theta^2}+\frac{\partial^2 \Phi}{\partial z^2}=4\pi G\rho(R,z).$$

If axial symmetry is assumed, and the rotation curve is flat, then,

$$\frac{1}{R}\frac{\partial}{\partial R}\left(R\frac{\partial \Phi}{\partial R}\right)+\frac{\partial^2 \Phi}{\partial z^2}=\frac{1}{R}\frac{\partial}{\partial R}(RF_R)+\frac{\partial^2 \Phi}{\partial z^2};$$

$$\frac{1}{R}\frac{\partial}{\partial R}(v_c^2)+\frac{\partial^2 \Phi}{\partial z^2}=\frac{\partial^2 \Phi}{\partial z^2}=4\pi G\rho(R,z),$$

where,

$$-\frac{\partial \Phi}{\partial R}=F_R=\frac{v_c^2}{R}.$$

Assuming that the isothermal sheet has an isothermal distribution function,

$$f = f(E_z) = \frac{\rho_0}{(2\pi\sigma_z^2)^{1/2}} e^{-E_z/\sigma_z^2},$$

where,

$$E_z = \Phi(z) + 1/2v_z^2$$

(note that the disk height << disk scale length), the density is thus,

$$\rho = \int_{-\infty}^{\infty} \frac{\rho_0}{(2\pi\sigma_z^2)^{1/2}} e^{-(\Phi+1/2v_z^2)/\sigma_z^2} dv_z = \rho_0 e^{-\Phi/\sigma_z^2}.$$

Poisson's Equation is thus,

$$\frac{\partial^2\Phi}{\partial z^2} = 4\pi G\rho_0 e^{-\Phi/\sigma_z^2}.$$

We can express the above equation in a non-dimensional form by making the following substitutions,

$$\phi = \Phi/\sigma_z^2 \quad \text{and} \quad \xi = z/z_0,$$

where,

$$z_0 = \left(\frac{\sigma_z^2}{8\pi G\rho_0}\right)^{1/2}.$$

Differentiating the substituted terms,

$$\sigma_z^2 d\phi = d\Phi \quad \text{and} \quad z_0 d\xi = dz.$$

Thus,

$$2\sigma_z^2 \frac{d^2\phi}{dz^2} = 8\pi G\rho_0 e^{-\phi};$$

$$2\frac{d^2\phi}{d(\frac{z}{(\sigma_z^2/8\pi G\rho_0)^{1/2}})^2} = e^{-\phi};$$

$$2\frac{d^2\phi}{d\xi^2} = e^{-\phi}.$$

From the density expression derived from the distribution function, ϕ can be substituted into the previous equation such that,

$$\ln \rho = \ln \rho_0 - \phi.$$

Thus,

$$2\frac{d^2\phi}{d\xi^2} = \frac{\rho}{\rho_0},$$

which has the solution,

$$\rho = \rho_0 \mathrm{sech}^2\left(\frac{\xi}{2}\right),$$

or,

$$\rho = \rho_0 \mathrm{sech}^2\left(\frac{1}{2}\frac{z}{z_0}\right).$$

From,

$$z_0 = \left(\frac{\sigma_z^2}{8\pi G \rho_0}\right)^{1/2},$$

we can solve for σ_z,

$$\sigma_z^2 = 8\pi z_0^2 G\rho_0.$$

If ρ_0 (i.e., $\rho_{z=0}$) at any radius, *r*, is an exponential function of *r*, then,

$$\sigma_z^2 \propto \rho_0 \propto e^{-r/r_0}.$$

Because of this, many have modified the surface brightness Profile equation to take into account the isothermal sheet Model,

$$I(r, z) = I_0 e^{-r/r_0} \mathrm{sech}^2(z/z_0).$$